Solvent-Directed Self-Assembly

DOI: 10.1002/ange.200601888

Application of Solvent-Directed Assembly of Block Copolymers to the Synthesis of Nanostructured Materials with Low Dielectric Constants**

*Thomas M. Hermans, Jeongsoo Choi, Bas G. G. Lohmeijer, Geraud Dubois, Russell C. Pratt, Ho-Cheol Kim, Robert M. Waymouth, and James L. Hedrick**

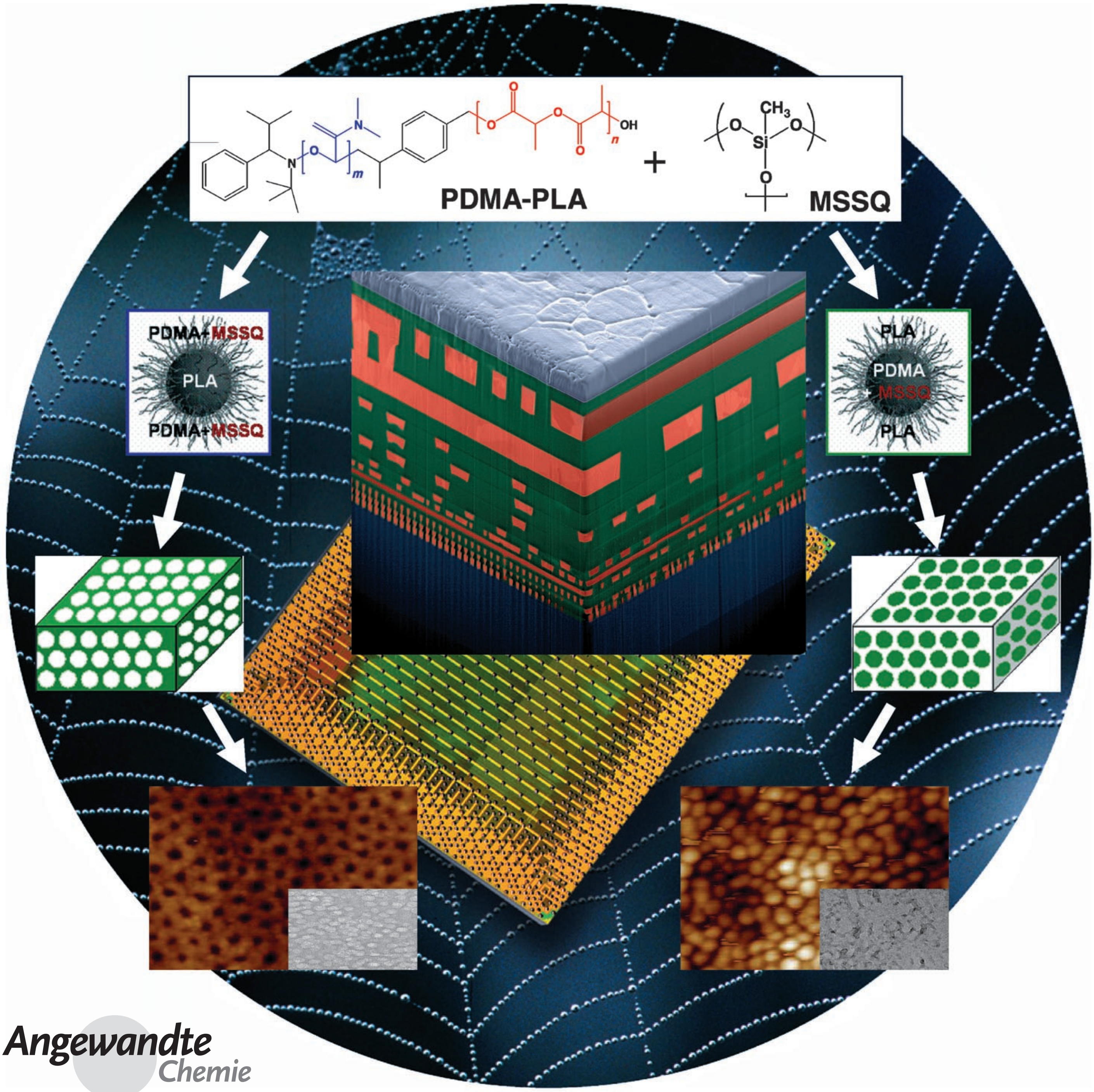

The pursuit of low-dielectric-constant, on-chip insulating media to mitigate both signal delays and power consumption for back-end of the line (BEOL) applications continues to be a challenge in the microelectronics industry.[1] A promising class of low-dielectric-constant materials are methyl silsesquioxanes (MSSQ) or organosilicates, and dielectric extendibility for future technologies (65- and 45-nm lithographic nodes) is through the controlled introduction of porosity. However, interconnectivity between the pores is obtained at a high level of porosity, which results in the contamination of the dielectric materials, including metal migration during processing, and subsequent degradation of the electrical properties.[2] The ability of a porous media to support high levels of porosity without percolation continues to be a grand challenge. In this regard, isolated pores with minimal interconnectivity have been generated through templating of organosilicates using star-shaped block copolymers[3] or dendrimers.[4,5] Nevertheless, the synthesis of these complex architectures is difficult. Another approach is based on the formation of a 3D cubic phase by the self-assembly of a diblock or triblock copolymer with a silica precursor.[6–11]

Here we describe a novel approach to highly porous hydrophobic MSSQ thin films with minimally interconnected porosity based on the co-assembly of organosilicate precursors with poly(*N*,*N*-dimethylacrylamide)-*block*-poly(*rac*-lactide) copolymer (PDMA-PLA). We also demonstrate that the deposition solvent plays a key role in directing the vitrification of the organosilicate, thus significantly expanding the range of accessible morphologies.[12–18] The use of PLA stems from its incompatibility with the organosilicate and thermal instability, as demonstrated by Hillmyer and Rzayev with the use of PLA copolymers to generate porous organic materials.[19,20] The nitrogen substitution in PDMA delivers characteristics commensurate with the formation of miscible blends with organosilicates, that is, polarity, hydrogen-bonding capability, and basicity, which promote strong interactions between the polymeric porogen and the thermosetting organosilicate precursors as described by Chujo and Saegusa.[21] The ability of the thermosetting organosilicate to be sequestered selectively into the PDMA phase allows preservation of the supramolecular assembly once cross-linked and results in a contiguous functional film. The utility of selectively cross-linking of the individual components of such self-assembled nanostructures has been shown by Wooley et al.,[22–24] who demonstrated stability, subsequent functionalization, and application in diverse environments. The distinguishing feature here is the use of a single block copolymer/organosilicate mixture that can generate widely different nanostructures simply by changing the deposition solvent.[12–18] A solvent selective for either the PDMA/MSSQ phase or PLA phase generates micellar or inverse micellar structures, respectively, followed by the preservation of the structure through organosilicate vitrification and copolymer burnout to give highly porous films with uniquely defined morphologies.

A series of poly(*N*,*N*-dimethylacrylamide)-*block*-polylactide block copolymers were prepared using Hawker's dual-headed initiator containing an alkoxyamine and a primary hydroxy group (Scheme 1).[25] Four hydroxy-terminated PDMA macroinitiators of various molecular weight were synthesized by nitroxide-mediated polymerization. Subsequent ring-opening of *rac*-lactide was accomplished by using a thiourea tertiary amine catalysts for bifunctional activation of both monomer and alcohol through hydrogen bonding.[26] Separating the tertiary amine functionality from the thiourea catalyst enabled us to increase polymerization rates without loss of control by addition of an auxiliary tertiary amine such as (−)-sparteine.[27] The versatility of this catalytic system is demonstrated through the synthesis of narrowly dispersed PLA blocks with predictable molecular weights (see Supporting Information). An example of the successful chain

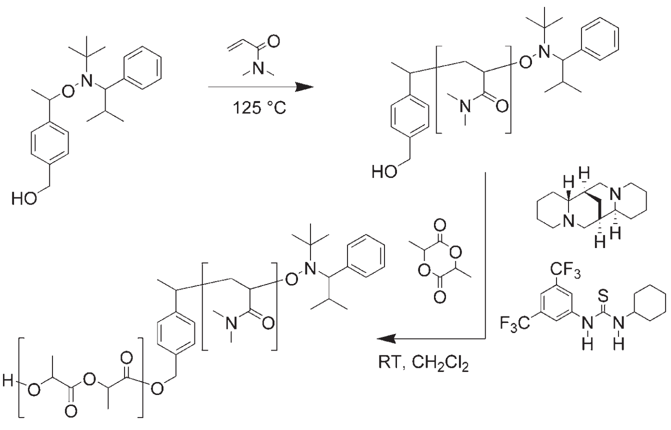

Scheme 1. Synthesis of PDMA-PLA block copolymers by sequential nitroxide-mediated and ring-opening polymerization.

---

[*] T. M. Hermans,[+] Dr. J. Choi,[+] Dr. B. G. G. Lohmeijer,[+]
Dr. G. Dubois, Dr. R. C. Pratt, Dr. H.-C. Kim, Dr. J. L. Hedrick
IBM Almaden Research Center
650 Harry Road, San Jose, CA 95120 (USA)
Fax: (+1) 408-927-3310
E-mail: hedrick@almaden.ibm.com
Prof. R. M. Waymouth
Department of Chemistry
Stanford University
Stanford, CA 94305 (USA)

[+] These authors contributed equally to this work.

[**] The authors acknowledge support from the NSF Center for Polymer Interfaces and Macromolecular Assemblies (CPIMA: NSF-DMR-0213618). This work was also partially supported by the Korea Research Foundation Grant funded by the Korean Government (MOEHRD) (KRF-2005-214-D00273). Part of this research was carried out at the Stanford Synchrotron Radiation Laboratory, a national user facility operated by Stanford University on behalf of the US Department of Energy, Office of Basic Energy Sciences. The SSRL Structural Molecular Biology Program is supported by the Department of Energy, Office of Biological and Environmental Research, and by the National Institutes of Health, National Center for Research Resources, Biomedical Technology Program. We thank M. Toney, H. Tsuruta, and M. Niebuhr for help with the SAXS experiments, and Leslie E. Krupp for the TEM studies. J.C. thanks Byeongdu Lee at Argonne National Laboratory for valuable assistance with the SAXS data analysis.

Supporting information for this article is available on the WWW under http://www.angewandte.org or from the author.

extension of the PLA block from the PDMA macroinitiator with no trace of homopolymer contamination is also shown in the Supporting Information. The volume fractions of the four PDMA-PLA block copolymers used for this study were very similar ($\phi_{\mathrm{PDMA}} \approx 0.25$) and facilitate comparison of structure–property relationships of the obtained organosilicate structures after polymer burnout.

When MSSQ resin and block copolymer **3** (PDMA$_{70}$-PLA$_{150}$, $M_n = 47\,100\ \mathrm{g\,mol^{-1}}$, PDI = 1.11) are dissolved in propylene glycol propyl ether (PGPE), a selective solvent for PDMA and a poor solvent for PLA, the solutions immediately manifest a blue glow, suggesting micelle formation. Using deuterated methanol as a model solvent, ^{1}H NMR spectroscopy shows that the signals associated with the PLA block are suppressed up to 60 °C, suggesting that PLA comprises the core of the micelle and is collapsed (see Supporting Information). Above 60 °C, the supramolecular structure is disrupted and leads to solvation, as shown by reacquisition of the ^{1}H NMR signals of the PLA block. Similarly, in the PLA-selective solvent *n*-butyl acetate (BuOAc) copolymers **1**–**4** show a blue glow as an indicator of micelle formation.

Thin films of hybrids containing approximately 60% (w/w) of a block copolymer, about 40% (w/w) MSSQ, and roughly 2% triethylamine (a catalyst for MSSQ condensation) were prepared by spin-coating both PGPE and BuOAc solutions (10% solids (w/w)) onto silicon wafers. The spin-coated films were annealed at 50 °C for 3 days to accelerate vitrification of the MSSQ while preserving the micellar structure, and then heated to 450 °C to degrade the polymer template out of the thin films.

Transmission electron microscopy (TEM) and field-emission scanning electron microscopy (FESEM) images together with the atomic force microscopy (AFM) image of the top surface of the mixture of MSSQ and copolymer **3** deposited from PGPE and BuOAc solutions are shown in Figure 1. In the case of the PGPE film, discrete, minimally interconnected pores are observed in the bulk of the film with a pore size of approximately 30 nm in diameter, and AFM measurements show analogous porosity on the surface. These structures are consistent with the imprinting of the micellar structure, with silica-free PLA comprising the core and the PDMA-MSSQ phase comprising the corona. The high final cure temperature allows the outer surfaces of the micelles to condense into a contiguous film, but the empty micellar cores are preserved to give a material that is highly porous with minimal interconnectivity. The refractive index and dielectric constant (*k*) of the porous material are 1.1825 and 1.71, respectively, values that are considerably lower than those for the dense organosilicate (1.3703 and 2.80, respectively). The density of the film material as determined from the critical angle of X-ray reflectivity (XRR) is 0.616 g cm^{-3}, which provides an estimate of the porosity as 52% when compared to the bulk material (1.273 g cm^{-3}). As the volume fraction of PLA is 45%, most of the porosity is believed to be derived from the space occupied by the PLA core.[28]

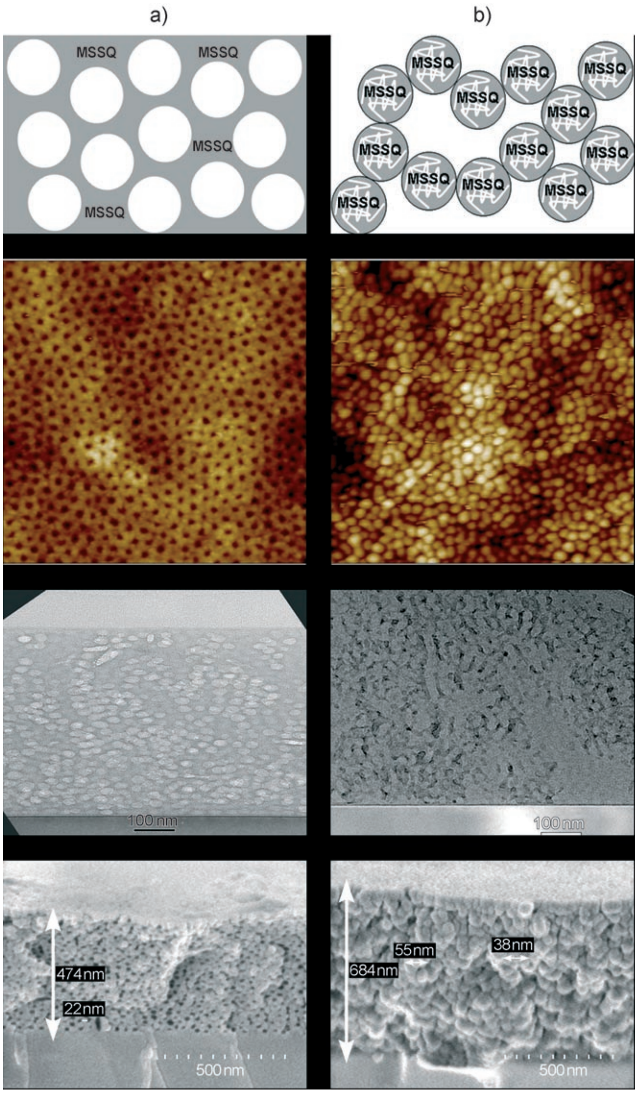

Figure 1. Micrographs of a) micellar and b) inverse micellar nanostructured thin films. Top: AFM images; middle: TEM images; bottom: FESEM images. See text for details.

A markedly different morphology is observed for the MSSQ/**3** mixture deposited from BuOAc and subsequently cured under the same conditions (Figure 1). The AFM micrographs show packed silica nanoparticles in both the bulk and on the surface. The exacerbated interstitial sites stem from the PLA phase that forms the corona of the nanoparticle precursors. The porosity was estimated at 64% (v/v) by XRR measurement (density: 0.456 g cm^{-3}) which corroborates the decrease in both the dielectric constant and refractive index to 1.65 and 1.13, respectively. The higher porosity implicates roles for both phases of the copolymer when BuOAc is used as the casting solvent. Although PDMA is miscible with MSSQ, curing causes phase separation of the PDMA component and subsequent formation of microporosity in the nanoparticles.[29,30] Pore generation therefore is reflected in both PLA-derived interstitial spaces and PDMA-derived inherent porosity of the nanoparticle matrix.

The microstructure of the porous films was investigated using small-angle X-ray scattering (SAXS). The 2D scattering image was integrated to 1D data after careful removal of background scattering. The reduced data were analyzed using the Pederson formalism[31] with a Schultz size distribution (see Supporting Information for details). Figure 2 a and b show the SAXS profiles as well as their fitted lines for thin films of MSSQ/**3** cast from PGPE and BuOAc, respectively. The characteristic SAXS profiles indicate that the pores in the thin films cast from PGPE are well-defined spheres, while the particles in the thin films cast from BuOAc are relatively deformed spheres. SAXS intensity profiles were further analyzed to characterize the structural features of thin films. From the extracted structure factor, $S(qr)$ (see Supporting Information), it was determined that the pores in thin films cast from PGPE form with a relatively ordered structure presumably in the manner of simple cubic (SC) or body-centered cubic (BCC) crystals, while the particles in thin films cast from BuOAc are not assembled into long-range-ordered structures. The deformation of the spheres and destruction of ordered structure in thin films cast from BuOAc may reflect the merging and respacing of the MSSQ particles upon thermolysis of the PLA phase.

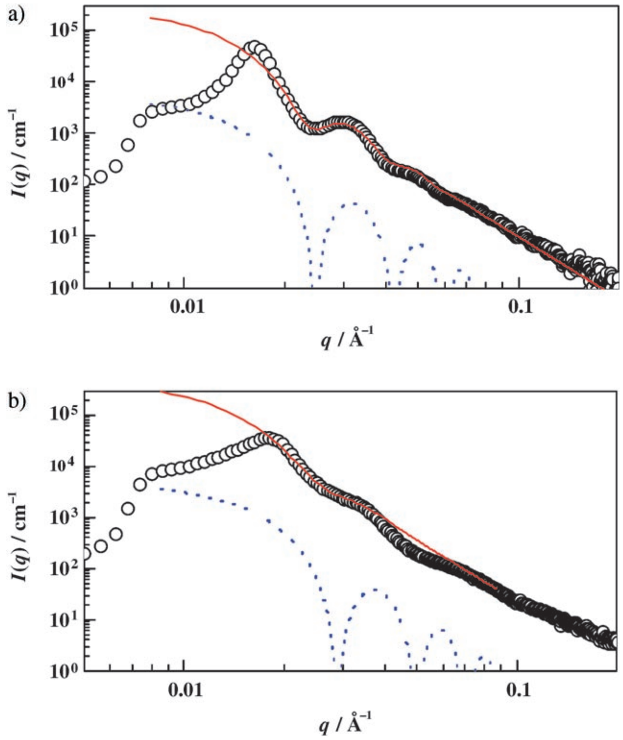

Figure 2. SAXS scattering profiles (symbols) and fits (solid lines) of thin film prepared from a) PGPE and b) BuOAc. Dotted lines show the scattering profiles calculated for monodisperse hard spheres, with the radius of gyration (R_g) being the average value in the distribution.

In summary, the co-assembly of organosilicate precursors with PDMA-PLA block copolymers deposited from solvents selective for either the PDMA or PLA phases was described. Mixtures deposited from PGPE produced a film with a dielectric constant of $k = 1.71$ and with discrete, minimally interconnected pores, while samples deposited from BuOAc generated contiguous films ($k = 1.47$) of packed, microporous nanoparticles. The simplicity of this strategy makes it attractive for application to future technology nodes.

Received: May 13, 2006

Keywords: block copolymers · micelles · porous materials · self-assembly · silicates

---

[1] J. L. Hedrick, T. Magbitang, E. F. Connor, T. Glauser, W. Volksen, C. J. Hawker, V. Y. Lee, R. D. Miller, *Chem. Eur. J.* **2002**, *8*, 3308.

[2] M. R. Baklanov, K. Maex, *Philos. Trans. R. Soc. London Ser. A* **2006**, *364*, 201.

[3] E. F. Connor, L. K. Sundberg, H. C. Kim, J. J. Cornelissen, T. Magbitang, P. M. Rice, V. Y. Lee, C. J. Hawker, W. Volksen, J. L. Hedrick, R. D. Miller, *Angew. Chem.* **2003**, *115*, 3915; *Angew. Chem. Int. Ed.* **2003**, *42*, 3785.

[4] B. Lee, Y. H. Park, Y. T. Hwang, W. Oh, J. Yoon, M. Ree, *Nat. Mater.* **2005**, *4*, 147.

[5] B. Lee, I. Park, J. Yoon, S. Park, J. Kim, K. W. Kim, T. Chang, M. Ree, *Macromolecules* **2005**, *38*, 4311.

[6] D. Zhao, P. Yang, N. Melosh, J. Feng, B. F. Chmelka, G. D. Stucky, *Adv. Mater.* **1998**, *10*, 1380.

[7] A. Jain, L. M. Hall, C. B. W. Garcia, S. M. Gruner, U. Wiesner, *Macromolecules* **2005**, *38*, 10095.

[8] A. Jain, G. E. S. Toombes, L. M. Hall, S. Mahajan, C. B. W. Garcia, W. Probst, S. M. Gruner, U. Wiesner, *Angew. Chem.* **2005**, *117*, 1252; *Angew. Chem. Int. Ed.* **2005**, *44*, 1226.

[9] A. Jain, U. Wiesner, *Macromolecules* **2004**, *37*, 5665.

[10] Y. Zhou, J. H. Schattka, M. Antonietti, *Nano Lett.* **2004**, *4*, 477.

[11] D. L. Gin, W. Q. Gu, B. A. Pindzola, W. J. Zhou, *Acc. Chem. Res.* **2001**, *34*, 973.

[12] K. J. Hanley, T. P. Lodge, C. I. Huang, *Macromolecules* **2000**, *33*, 5918.

[13] T. P. Lodge, B. Pudil, K. J. Hanley, *Macromolecules* **2002**, *35*, 4707.

[14] R. Glass, M. Moller, J. P. Spatz, *Nanotechnology* **2003**, *14*, 1153.

[15] J. F. Gohy, E. Khousakoun, N. Willet, S. K. Varshney, R. Jerome, *Macromol. Rapid Commun.* **2004**, *25*, 1536.

[16] J. F. Gohy, N. Willet, S. Varshney, J. X. Zhang, R. Jerome, *Angew. Chem.* **2001**, *113*, 3314; *Angew. Chem. Int. Ed.* **2001**, *40*, 3214.

[17] I. I. Potemkin, M. Moller, *Macromolecules* **2005**, *38*, 2999.

[18] G. Riess, *Prog. Polym. Sci.* **2003**, *28*, 1107.

[19] J. Rzayev, M. A. Hillmyer, *Macromolecules* **2005**, *38*, 3.

[20] J. Rzayev, M. A. Hillmyer, *J. Am. Chem. Soc.* **2005**, *127*, 13373.

[21] Y. Chujo, T. Saegusa, *Adv. Polym. Sci.* **1992**, *100*, 12.

[22] H. Y. Huang, E. E. Remsen, T. Kowalewski, K. L. Wooley, *J. Am. Chem. Soc.* **1999**, *121*, 3805.

[23] Q. G. Ma, E. E. Remsen, T. Kowalewski, K. L. Wooley, *J. Am. Chem. Soc.* **2001**, *123*, 4627.

[24] K. K. Perkin, J. L. Turner, K. L. Wooley, S. Mann, *Nano Lett.* **2005**, *5*, 1457.

[25] C. J. Hawker, A. W. Bosman, E. Harth, *Chem. Rev.* **2001**, *101*, 3661.

[26] A. P. Dove, R. C. Pratt, B. G. G. Lohmeijer, R. M. Waymouth, J. L. Hedrick, *J. Am. Chem. Soc.* **2005**, *127*, 13798.

[27] R. C. Pratt, B. G. G. Lohmeijer, D. A. Long, P. N. P. Lundberg, A. P. Dove, H. Li, C. G. Wade, R. M. Waymouth, J. L. Hedrick, unpublished results.

[28] A total of 55% (v/v) porosity is expected according to an independent experiment using 15% (w/w) PDMA ($M_r = 7000$) wherein 10% (v/v) porosity was obtained.

[29] D. Mecerreyes, E. Huang, T. Magbitang, W. Volksen, C. J. Hawker, V. Y. Lee, R. D. Miller, J. L. Hedrick, *High Perform. Polym.* **2001**, *13*, S11.

[30] R. D. Miller, W. Volksen, V. Y. Lee, E. Connor, T. Magbitang, R. Zafran, L. Sundberg, C. J. Hawker, J. L. Hedrick, E. Huang, M. Toney, Q. R. Huang, C. W. Frank, H. C. Kim in *Polymers for Microelectronics and Nanoelectronics*, ACS Symposium Series 894, ACS, Washington DC, **2004**, pp. 144.

[31] J. S. Pedersen, *J. Appl. Crystallogr.* **1994**, *27*, 595.